Accepted Manuscript

Wire bonding on glass substrates via vapour deposition of Ag-Ti film

Nicholas Kam, Michael David Hook, Tanya Tang, Michael Mayer

PII: S0026-2692(18)30974-1

DOI: https://doi.org/10.1016/j.mejo.2019.05.009

Reference: MEJ 4552

To appear in: *Microelectronics Journal*

Received Date: 14 December 2018

Revised Date: 3 May 2019

Accepted Date: 15 May 2019

Please cite this article as: N. Kam, M.D. Hook, T. Tang, M. Mayer, Wire bonding on glass substrates via vapour deposition of Ag-Ti film, *Microelectronics Journal* (2019), doi: https://doi.org/10.1016/j.mejo.2019.05.009.

Wire Bonding on Glass Substrates via Vapour Deposition of Ag-Ti Film

Nicholas Kam, Michael David Hook, Tanya Tang, Michael Mayer
University of Waterloo, 200 University Ave. W., Waterloo, ON N2L 3G1 Canada
Ph: 519-888-4567, Ext. 38579
Email: nkam@uwaterloo.ca

Abstract

Circuits on glass technology have recently developed in applications such as interposers, fibre optics, and displays. We report an automatable method towards interconnecting to glass circuits via wire bonding with maintained transparency. The method is based on wire bonding Au-Ag, using 25 µm diameter 99.99 % pure Au wire. A 5 nm Ti and 500 nm Ag base film are initially deposited via e-beam evaporation onto a standard glass slide, where after wire bonding is preformed. The metal film is then etched from the substrate via ion-milling; remaining intact only in areas shielded from the beam. Cross-sections of the bonded balls before and after metallization removal show high quality continuous interfaces with no intermetallic or micro void formations. Good reliability was indicated by shear testing, remaining above 100 MPa for at least 8 days of ageing at 200 °C. Strong wire bonds were thus obtained on a glass substrate by deposition and selective removal of a Ag-Ti film.

Introduction

Glass is a versatile material suitable for electrical applications due to its excellent isolating capabilities and mechanical properties [1] [2]. Pure glass (e.g. fused silica) proves to have superior thermomechanical, dielectric, and optical properties to many ceramics.

Recent developments in technology has reintroduced glass in various electronic applications. Glass interposers used as building blocks for 3D-integrated circuits (ICs) have enabled high density packing with through silicon via technology [3]. Glass interposers allow for smaller feature sizes than organic substrates due to better dimensional stability, and are less expensive than those made from monocrystalline silicon [4]. For parallel interconnection, a metallized glass substrate was demonstrated with parallel lines between two integrated circuit chips using flip chip bonding technology [5]. A non-transparent electroplated Cr/Au sandwich was used as metallization. In applications such as liquid crystal displays that require transparent components, a glass substrate with metal circuitry allows greater integration of optical and electronic components, as in chip on glass (COG) technology [6,7]. A reliable method for interconnecting on glass substrates is thus in increasing demand.

Wire bonding has been the most important interconnect technology for integrated circuits due to its versatility and low-cost. For bonding on glass substrates alternative methods based on anisotropic conductive adhesives is typically used [10]. Wire bonding is not popular in this application as it usually requires metal deposition with a subsequent patterning step prior to bonding.

Here an automatable wire bonding method is reported that requires no dedicated patterning process step. The proposed method consists of a vapour deposited metallization process, a Au-Ag wire bonding process, and a demetallizing stripping process.

Section I

1.1 Materials Selection and Process Design

The process diagram for bonding Au wires on glass is illustrated in Figure 1. Each process step is described in more detail in the following sections. A widely used 99.99% pure (4N) 25 µm diameter Au wire was chosen for bonding due to its high consistency, ease of process setup, and good bond reliability.

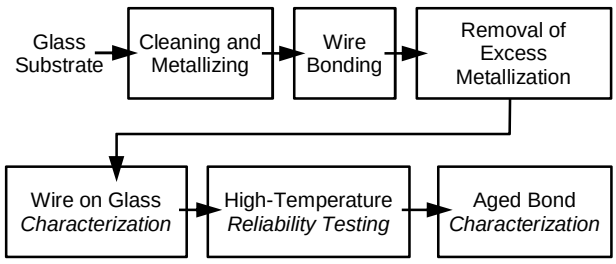

Figure 1: Flow diagram of process for sample preparation, testing, and characterization. Boxes in the top row are for sample preparation, bottom row are for testing and characterization.

The substrate used is a standard glass microscope slide (75 mm x 25 mm), made of soda-lime glass consisting largely of SiO_2. For novel low-cost processes it is useful to accelerate prototyping with lower-cost material. Ag was chosen as the top metallization layer for its good bondability and reliability with wire made from other noble metals. Ag oxidizes in an open environment; however, the

oxide conductivity can still be sufficient in some applications or easily removed through thermal decomposition above ≈ 200 °C. Ag does not adhere well directly to glass, so Ti was chosen as an adhesion layer due to its reactive nature that allows chemical bonding to SiO_2, resulting in strong adhesion [9].

1.2 Substrate Metallization by Vapour Deposition

The application of vacuum e-beam deposition of the Ag-Ti films benefits from reduced defects, vacancies and impurities during formation, which will result in a slower rate of interdiffusion during reliability testing and ageing [11]. Substrate cleaning was performed to achieve strong adhesion to the depositing film. The process flow for substrate cleaning and Ti/Ag deposition is illustrated in Figure 2.

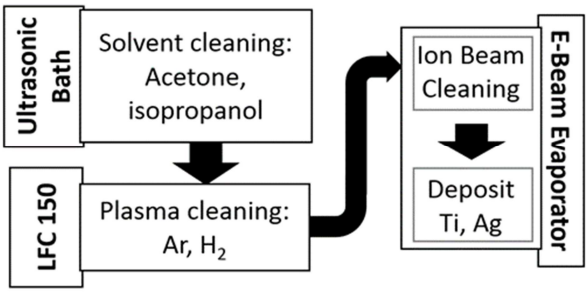

Figure 2: Flow diagram showing cleaning and metallization process steps for soda-lime glass substrate, split by equipment used.

To prepare the substrates for metallization a preliminary cleaning step was carried out to avoid gross contamination of the e-beam evaporation chamber in the subsequent process steps. The substrates were ultrasonically cleaned in a bath of acetone, a second bath of isopropanol, and then dried using pressurized nitrogen gas. Next, using a LFC150 G plasma cleaning system produced by samco-ucp (Ruggell, Liechtenstein), the substrates were plasma cleaned for 10 min using argon-hydrogen plasma to remove any organic thin films on the substrate. Finally, the substrates were cleaned for 15 min using pure argon plasma, using a Nanochrome II e-beam evaporator produced by Intlvac (Halton Hills, Ontario, Canada). This final cleaning step removes any contamination occurring from exposure to laboratory air. The substrates then remain under vacuum inside the chamber of the evaporator for the metal film deposition.

Ag-Ti deposition by e-beam evaporation is carried out in situ without further exposure to air. A 5 nm thick Ti film followed by a 500 nm thick Ag film are deposited by e-beam evaporation using the Nanochrome II. Deposition rates were set at Ti: 0.05 nm/s and Ag: 0.2 nm/s. The final metallized substrate is shown in Figure 3.

A Dektak stylus profilometer was used to study surface roughness of one substrate after metallization. The results are shown in Figure 4. The mean roughness was $R_a = 5.0$ nm.

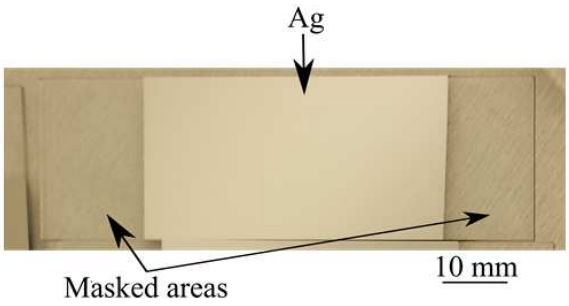

Figure 3: Photograph of Ag-Ti metallized glass slide. The ends of the substrate were masked by adhesive polyimide tape (Kapton tape) to secure in place during deposition.

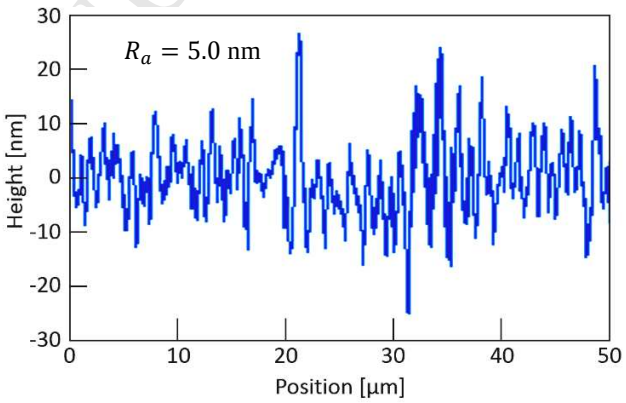

Figure 4: Surface roughness of Ag-Ti film measured by a Dektak mechanical profiler.

1.3 Wire Bonding

Bonding was performed with 25 µm diameter Au wire using an ESEC 3088 automatic ball bonder, machine parameters listed in Table 1. Parameter values were optimized for Au-Ag bonding using methods developed by Gomes et al. [12]. Test bonds were made in a grid pattern with 360 wire bonds on each of 4 substrates.

Bonded ball geometries were measured using an optical microscope. The bond zone area was calculated from average ball bond diametric measurements (Figure 5). Shear testing values were divided by the bond zone area to determine the final shear strength. Responses for the ball bonds prior to film removal are given in Table 2.

Table 1: Parameters used for wire bonding process on ESEC 3088 equipment. Wire material was Au.

Parameter	Value
Wire Diameter (μm)	25
Ball Impact Force (mN)	424
Ball Bond Force (mN)	185
Ball Bond Time (ms)	9.8
Ball Ultrasonic Power (%)	25.01
Ball Pre-Ultrasound (%)	10.01
Wedge Impact Force (mN)	350
Wedge Bond Force (mN)	350
Wedge Bond Time (ms)	9.8
Wedge Ultrasonic Power (%)	15.00
Wedge Pre-Ultrasound (%)	12.02
EFO Time (ms)	2.20
EFO Current (mA)	20.04
Temperature (°C)	200

Table 2: Mean ball bond process response before and after film removal via ion-milling. Standard deviation given.

Response	Before Demetallization	After Demetallization
Ball Height (BH) [µm]	24.6 ± 0.56	24.2 ± 0.61
Ball Diameter (BDC) [µm]	58.73 ± 0.73	57.95 ± 0.75
Ball Ovality (%)	6 %	5 %
Shear Force (SF) [mN]	27.77 ± 2.93	26.84 ± 3.77
Shear Strength (SS) [MPa]	100.6 ± 11.25	99.7 ± 13.01

1.4 Removal of Metallization by Ion-milling

To restore transparency to the glass substrate the Ag-Ti film must be removed with a process that leaves the metallization at the bonded areas intact to maintain bond integrity. The film must be completely removed everywhere else, particularly below the wire loops.

Typical methods for removal of thin metallic films, wet chemical etching and reactive ion etching (RIE), are not suitable for this application. Wet chemical etching was rejected as there was no available chemical that could remove the Ti film without severe attack to the metallization below the bonds, resulting in loss of bond strength and bonds popping off. RIE was rejected due to equipment contamination concerns arising from etching Au and Ag.

Instead, an ion-mill etching process was applied using a model ATC-2030-IM machine produced by AJA International, Inc. (Scituate, MA, USA). Parameters were set for an etching time of 30 min using an ion beam voltage of 400 V and current of 190 mA.

During ion-milling the sample holder was slowly rotated about its axis and tilted in steps to allow the beam to hit the substrate at angles of 15°, 30°, and 45° from perpendicular at different times. This rotation and tilting ensured that the ion beam reached under the central section of each wire loop, leaving no shadowed areas with residual metallic film.

No observable damage to the ball bonds was found after ion-milling, see Figure 5.

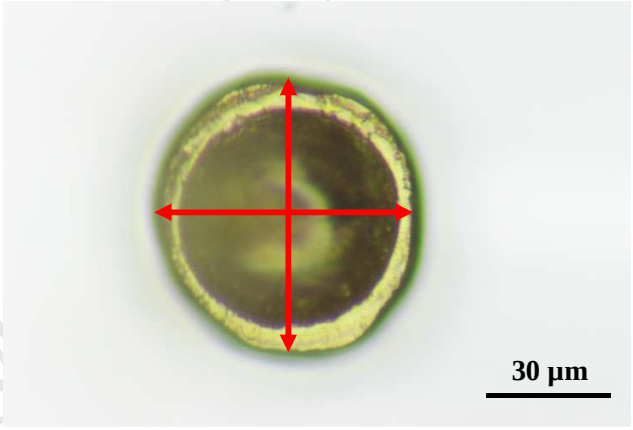

Figure 5: Optical image of a ball bond after ion-mill removal of metallized film. Bond area measurements shown.

The individual process steps: film deposition, wire bonding, and film removal by ion-milling, are all themselves automatable processes widely used in the electronics industry. This method of interconnecting onto glass substrates can therefore be easily integrated to large-scale manufacturing systems.

Section II

2.1 Affect of Metallization Stripping on Ball Bonds

Final bonds after film removal are shown in optical images Figure 6 (a) and (b). The ion-mill etching was sufficient to leave no visible Ag or Ti residue on the glass surface, restoring the substrate to its original transparency. No noticeable thinning of the wires was observed. Comparing the bonding response before and after ion-milling in Table 2, ball bond geometry and strength remained consistent throughout the process. A Student's t-test was performed on the shear responses before and after film removal. The test returned a p-value of 0.87, indicating no statistically significant difference between the shear strength means of the two of wire bonds sets.

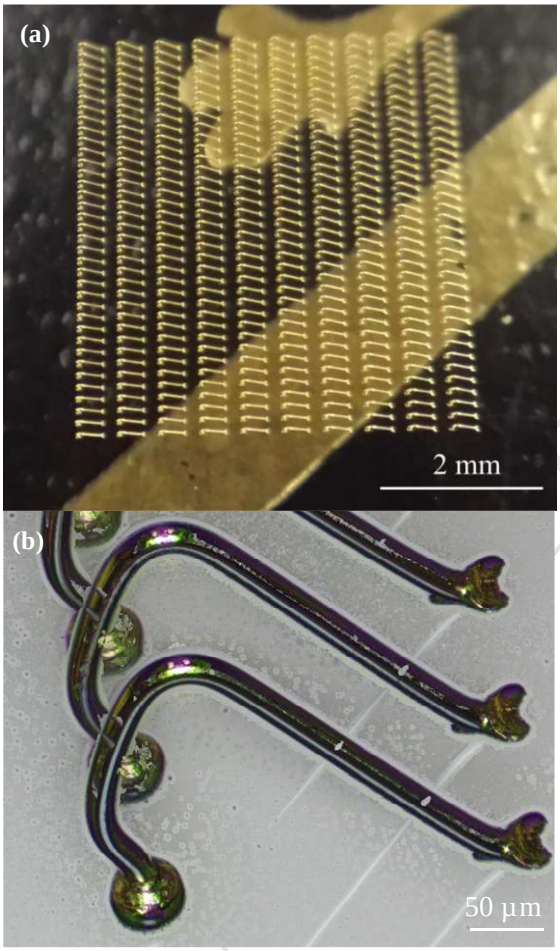

Figure 6: Wires on glass substrate after removal of Ag-Ti film by ion-milling. (a) Wires appear to float over the leather cover of a laboratory log book on which the transparent glass substrate is placed. (b) Optical close-up obtained using extended focus image capture.

SEM images of bonded ball cross-sections before and after film removal are shown in Figure 7 (a) and (b). After ion-milling, the Ag-Ti film remains only in regions shadowed by the ball. A close-up in Figure 7 (c) shows continuous interfaces between wire-metallization and metallization-glass. The micrograph shows no microvoids or intermetallics, indicating a sound ball bond. Moreover, the process was robust as a 100 % bonding yield was achieved.

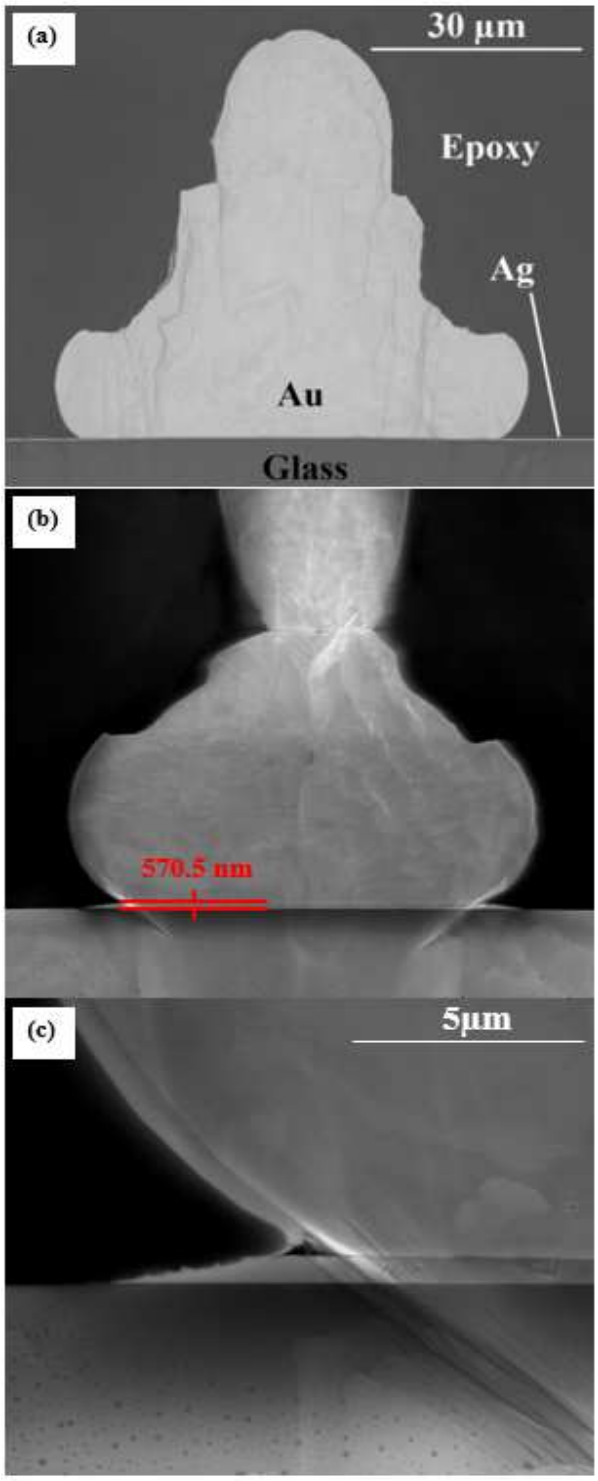

Figure 7: SEM showing a cross-section of a bonded Au ball bonds on a glass slide (a) with metallization, (b) after ion-milling, and (c) close-up of the ball bond-substrate interface.

2.2 Wire Bonds under High Temperature Storage

While the reliability of Au wire bonds to Ag metallization on Cu leadframes is well-established [11], the reliability is not yet confirmed for bonds on the Ag metallized glass. Reliability tests were performed using bonded substrates placed in an oven at 200 °C for 15 days. Shear testing was performed on bonds (n=20) prior to and after periods of 1 day, 8 days, and 15 days of ageing. Shear test results are box plotted in Figure 8.

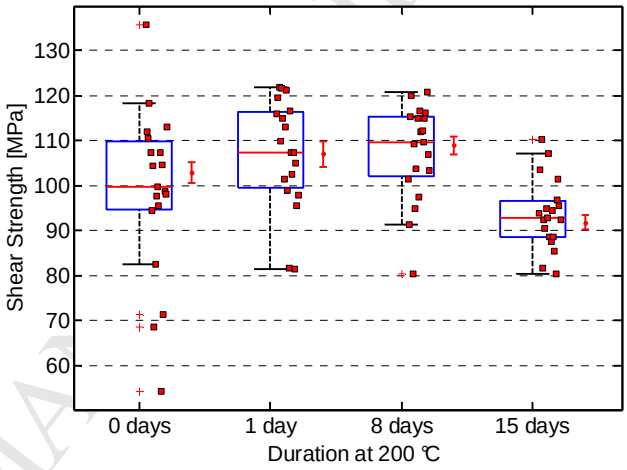

Figure 8: Shear strength box plots of Au ball bonds on Ag metallized glass after high temperature storage at 200 °C. Data set included as red squares, with outliers marked with an adjacent red cross. Means are marked next to box plots (red whiskers) with error bars (outliers removed).

The statistical minimum shear strength shown in the plot indicates that bond strength was maintained above 80 MPa for all days, demonstrating reliable bonding after ageing [11]. Mean shear strength response increased during the first 8 days, followed by a significant drop off after 15 days. The reduced strength is likely a result of adhesive degradation between the Ag-Ti film and glass substrate, discussed further in Section 2.3.

Standard deviation was found to be reduced after each ageing period; a result of possible minor weak bond healing due to the high temperature. For Au-Ag bonding, rapid diffusion of Ag into Au is known to occur at high temperatures above 150 °C, as determined by James [13] The primary mechanism of Ag diffusion into Au is noted to be grain boundary diffusion, which would impede dislocations within the Au ball crystal structure, improving its shear strength. This effect could account for the reduced deviation observed during the first 8 days of ageing.

2.3 Modes of Failure

Optical images of the ball bond shear interface after high temperature testing are shown in Figure 9.

Immediately after bonding, Figure 9 (a), failure occurs largely due to shearing through the bonded ball, as evident by the remaining Au layer at the shear site. The Ag-Ti film adhesion to the glass substrate therefore demonstrates a higher shear strength than the bulk Au wire material.

After ageing at high temperature, Figure 9 (b), failure appears to occur most frequently by delamination at the film-glass interface. The film adhesion after high temperature ageing appears to degrade and becomes the limiting strength factor for the bond during shear testing. This would account for the decreased shear strength seen after 15 days ageing.

Titanium film adhesion has been shown to increase when aged at high temperature due to its high affinity for oxygen and the increased thermal diffusion [14]. It is therefore possible that delamination occurs between the Ag and Ti interface due to intermetallic formation and phase structure transformations caused by thermal ageing.

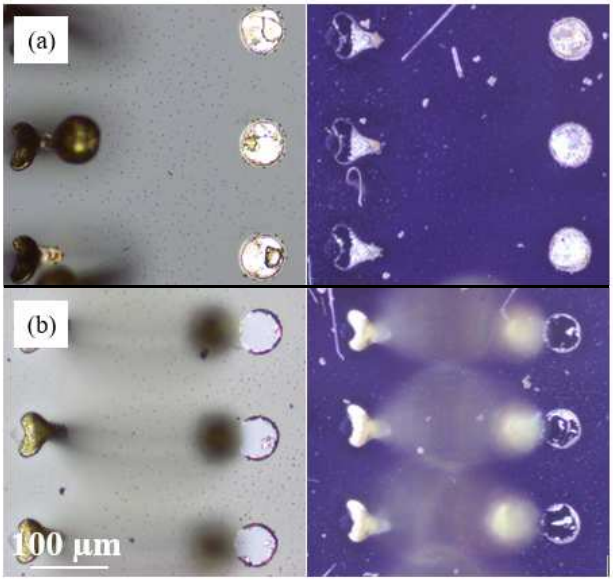

Figure 9: Optical micrographs of typical shear interfaces for Au bonds (a) immediately after bonding (b) and after ageing 15 days. Bright field images (left) compared against dark field (right) highlights delamination of Ag film after ageing.

Conclusions

Reliable Au ball-wedge bonds were demonstrated on a glass substrate using a vapour deposited a Ag-Ti interlayer as a wire bonding surface. Where optical transparency is required, the Ag-Ti film can be removed by ion-mill etching without apparent damage to the glass surface or change to the ball bond properties. The method described here can be applied to other interconnections on glass substrates. This method can also be replicated for wire bonding on other non-conductive surfaces compatible with Ag-Ti film deposition.

While the bonds remain strong after moderate high temperature storage, further study is needed to identify degradation mechanisms at the wire-to-film and film-to-glass interfaces during extended ageing times if higher reliability is required.

Additional work is needed to optimize the wedge bond process to minimize applied stress and maximize reliability, which is outside the scope of this work. Alternatively, wedge bonding directly on the Ag film may be avoided by using the “bond stitch on bump” (BSOB) technique.

Acknowledgments

We acknowledge financial support from Microbonds, Inc. and the National Science and Engineering Research Council (NSERC) of Canada. We are grateful for the use of equipment at the University of Waterloo in the Centre for Advanced Materials Joining, the Quantum NanoFab, and WATLab. This infrastructure would not be possible without the significant contributions of CFREF, CFI, Industry Canada, the Ontario Ministry of Research & Innovation and Mike & Ophelia Lazaridis. Their support is gratefully acknowledged.

References

1. Garner, S. M. (Ed.). (2017). Flexible Glass: Enabling Thin, Lightweight, and Flexible Electronics. John Wiley & Sons.
2. Phoenix, A. Z. (2014). Flexible glass: Enabling the future of electronics. In Cynthia Giroux, Flex 2014 Conference (pp. 3-6).
3. S. Kuramochi, H. Kudo, M. Akazawa, H. Mawatari, M. Tanaka and Y. Fukuoka, "Glass interposer technology advances for high density packageing," 2016 IEEE CPMT Symposium Japan (ICSJ), Kyoto, 2016, pp. 213-216.
4. V. Sukumaran, Q. Chen, F. Liu, N. Kumbhat, T. Bandyopadhyay, H. Chan, S. Min, C. Nopper, V. Sundaram and R. Tummala, "Through-package-via formation and metallization of glass interposers," in Proceedings 60th Electronic Components and Technology Conference (ECTC), Las Vegas, NV, USA, 2010.
5. L.-W. Pan, P. Yuen, L. Lin and E. Garcia, "Flip chip electrical interconnection by selective electroplating and bonding," Microsystem Technologies, vol. 10, no. 1, pp. 7-10, 2003.
6. M. Masuda, K. Sakuma, E. Satoh, Y. Yamasaki, H. Miyasaka and J. Takeuchi, "Chip on glass technology for large capacity and high resolution LCD," in Sixth IEEE/CHMT International Electronic Manufacturing Technology Symposium, 1989.

7. R. Joshi, "Chip on glass—interconnect for row/column driver packageing," Microelectronics Journal, vol. 29, no. 6, pp. 343-349, 1998.
8. T. Budka, "Wide-bandwidth millimeter-wave bond-wire interconnects," IEEE Transactions on Microwave Theory and Techniques, vol. 49, no. 4, pp. 715-718, 2001.
9. D. Adams and T. L. Alford, Silver Metallization: Stability and Reliability, Springer, 2008, p. 1.
10. S.-H. Lee, T.-W. Kim, K.-L. Suk and K.-W. Paik, "Nanofiber Anisotropic Conductive Films (ACF) for Ultra-FinePitch," Journal of Electronic Materials, vol. 44, no. 11, p. 4628–4636, 2015.
11. G. Harman, Wire Bonding in Microelectronics, McGraw-Hill, 2010.
12. J. Gomes, M. Mayer and B. Lin, "Development of a fast method for optimization of Au ball bond process," Microelectronics Reliability, vol. 55, pp. 602-607, 2015.
13. K. James, “Reliabilty Study of Wire Bonds to Silver Plated Surfaces,” I2EEE Trans. on Parts, Hybrids and Packageing, vol. 13, pp. 419-425, 1977.
14. Benjamin, P., & Weaver, C. (1961). The Adhesion of Evaporated Metal Films on Glass. Proceedings of the Royal Society of London. Series A, Mathematical and Physical Sciences, 261(1307), 516-531